StarNav III: A Three Fields of View Star Tracker[1][2]

Daniele Mortari[1], and Andrea Romoli[2]
[1] Università degli Studi "La Sapienza" di Roma
Via Salaria, 851 - 00138 Roma (Italy)
+39 (06) 88346-432, mortari@psm.uniroma1.it
[2] Alenia Difesa - Unità Officine Galileo
Via Einstein, 35 - 50013 Campi Bisenzio (Italy)
+39 (055) 8950-550, andrea.romoli@officine-galileo.finmeccanica.it

Abstract—Italian Space Agency has funded, as one of the possible Italian experiment on board the International Space Station, the development of a new star tracker, called StarNav III, which observes the sky by means of three orthogonal fields of view and focuses all the star images onto a single CCD/CMOS imager. The main characteristics of this sensor are a high gain in the attitude accuracy estimation and in the operating time. These benefits cost, however, in terms of hardware and software design which are, in turn, more complex. The StarNav III feasibility study, recently completed, has output a variety of new software approaches (as, for instance, for acquisition, centroiding, star identification, and mirror misalignment), most of which can directly be applied to almost all of the existing CCD/CMOS star trackers. This paper shows the principal aspects of the relevant feasibility study.

TABLE OF CONTENTS

1. INTRODUCTION

The idea of increasing both accuracy and operating time of star trackers by splitting the observable sky into orthogonal additional Fields of View (FOV), was detailed discussed in [1], even though [2] first presented the idea of splitting FOV camera. The idea consists of imaging, by means of a proper optical system, the stars observed in two/three orthogonal directions into a single CCD/CMOS. In this way, two critical problems for star trackers are solved. Namely, due to the fact that the attitude accuracy is polarized toward the FOV Optical Axis (there is a difference of an order of magnitude between the accuracy along and about the OA direction), and the fact that if the Sun, or the Earth, or the Moon falls into the sensor FOV, the instrument cannot be operative.

The three FOVs StarNav III star tracker is, like the dual FOVs StarNav II, presented in [1,3-5,12], designed to provide a high gain in term of attitude accuracy and operating time with respect to an equivalent, single FOV, star tracker.

The StarNav III feasibility study, which was completed by September 2001, contains many new interesting aspects in both hardware and software developed. In particular, most of the proposed data processing to accomplish acquisition, centroiding, star identification, and attitude estimation, can directly be adopted by almost all of the CCD star trackers to improve accuracy and speed of the associated data processing. This paper contains discussions on these new hardware and software aspects by showing the advantages, disadvantages, and feasibility of each proposed solution.

As for the hardware, the optical solution proposed by the Italian industry Officine Galileo (Alenia Difesa) consists of a Schmidt-Cassegrain catadioptric system designed with a geometrical partition of the pupil area. This system, by means of three sets of mirrors, whose perpendicular directions constitute an orthogonal set of directions, allows us to project the observed stars of all the three FOVs on a single imager. In this way, the resulting optical system is a Schmidt-Cassegrain lens which has an accessible input pupil and, therefore, tends to become telecentric in input.

However, the fact that the stars coming from different FOVs are focused onto a single CCD, introduces the problem to keep the FOV info, that is, the need of performing, in some way, the FOV identification. This implies to develop a procedure to understand the correspondence between the CCD spot lights and the FOV of provenance. This paper presents three different ways (one chromatic and two monochromatic) to solve this problem, that is, to identify from which, of the three FOVs, the observed star belongs.

An important new approach has been proposed and developed to accomplish the centroiding process by means

0-7803-7231-X/01/$10.00/© 2002 IEEE
[2] IEEEAC paper #050, Updated November 29, 2001

of recursive functions and adaptive masks, and a dramatically robust algorithm for star identification (called *Pyramid III*), capable of quantifying the reliability of the star identification process, has also been developed. The latter new approach, which is based on an analytical theory [11], uses the recent *k*-vector method, firstly presented in [6] and generalized in [7], to solve the general range searching problem and identify the stars in the *lost-in-space* case, that is, when no attitude information is available. These new ideas will benefit, by implying substantial improvement in accuracy and computational speed, almost all star trackers.

2. Optics for Multifield Star Trackers

2.1 Multiple field optics

There are a few ways to conceive an optical system suitable for multiple FOV star trackers with only one common matrix detector. This optics shall be capable to solve two basic problems: the first is how to image two or more FOVs on the same detector, while the second is how to distinguish objects of a given FOV from that belonging to the others. For StarNav III the optics configuration was studied by means of first order analysis, focusing the attention on pupil partition, while some methods to render the system able to distinguish the FOVs will be explained.

2.2 Pupil partition

One simple way able to achieve the overlapping of two distinct FOVs on the same focal plane, is the use of a beam splitter placed in front of an objective, as done for the dual FOVs StarNav II sensor [4], and sketched in Fig. 1.

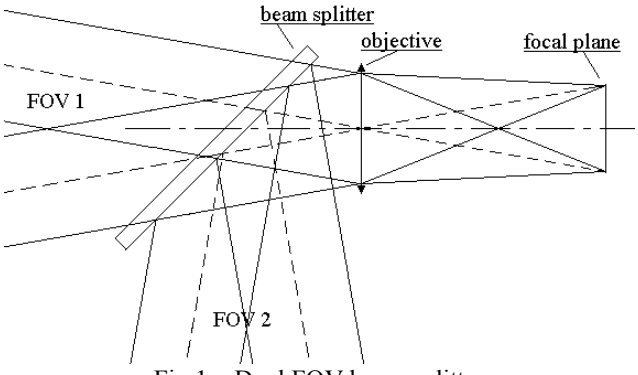

Fig.1 – Dual FOV beam splitter

The beam splitter reflects less than 50% of energy and transmits less than 50%. So the equivalent F/number is about two time higher than that of a single FOV star tracker. This loss of energy seems to be unavoidable, having two or more FOVs overlapped. Then both FOVs have to be marked in some way, chromatically, for instance, or introducing different amounts of aberration in each FOV.

Another way, more general, to achieve the overlapping of the two or more FOVs is to operate a pupil partition of energy. The idea consists in a geometrical FOV splitting in the pupil of an optical system by means of flat mirrors.

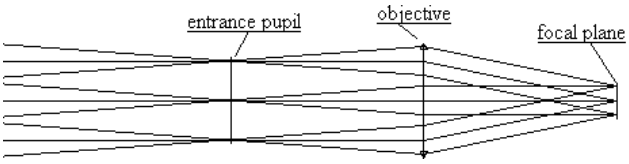

Fig. 2 – Telecentric objective

The condition which has to be satisfied to do this, is that the pupil position, common to each FOV, is located in front of the objective, at a suitable distance, in such a way that a pyramid of mirrors can be put on it, without optical and mechanical interference with the objective elements. In order to satisfy this condition the objective should be telecentric from the image side, i.e. its exit pupil has to be at infinity, as it is shown in Fig.2.

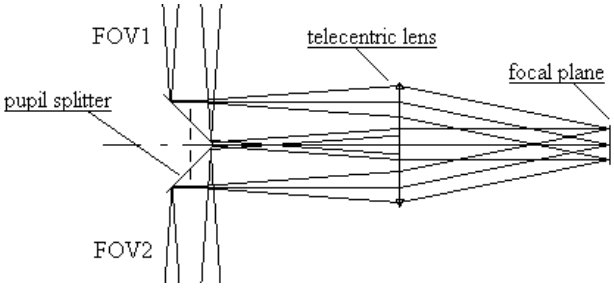

Fig. 3 – Pupil splitting with a telecentric lens

Using a concept similar to that shown in Fig. 3, the second author of this paper has found an optical system suitable for pupil splitting. It's based on a Schmidt-Cassegrain objective, like that shown in Fig.4.

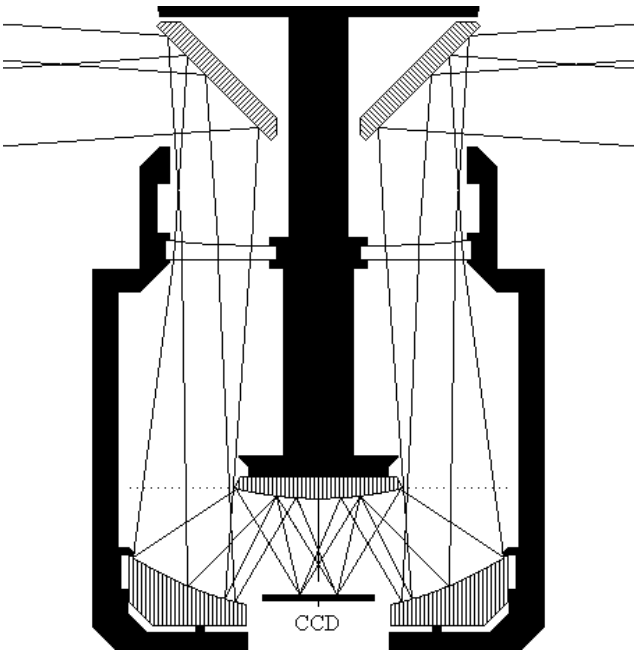

Fig. 4 – Schmidt-Cassegrain layout for StarNav III sensor

This objective is suitable for some 3-FOV configurations also, with two fields at 120° and the third orthogonal to the others, this last being obtained by removing the related folding mirror. The F/number for a three FOV sensor is about 3. The recognition of the FOV can be done taking advantage of the typical shape contour of the Point Spread Function (PSF). Indeed, all the PSF belonging to a FOV have similar shapes almost symmetrical to an axis which is oriented at 120° with respect to the others.

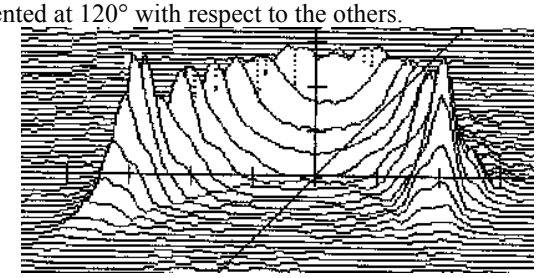

Fig. 5 – Typical PSF profile of the Schmidt-Cassegrain objective for one FOV

A typical PSF is shown in Figs. 5 and 6, while Fig. 7 shows the same PSF coming from another FOV. Due to the pupil partition, each FOV presents PSFs which tend to have a symmetry axis oriented at 120° with respect to other two FOVs. This situation is schematized in Fig. 8, where the PSFs of the three FOVs (A, B, and C) are represented.

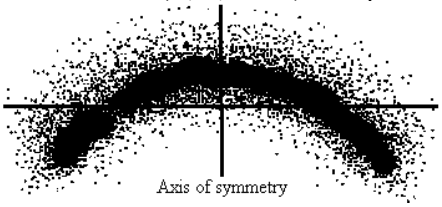

Fig. 6 – PSF intensity map

One can take advantage of this typical characteristic in order to roughly evaluate the PSF symmetry axis direction, with a simple mathematical algorithm, shown later. The found direction is related to the FOV to which the PSF belongs. Other algorithms can be used to determine the centroiding coordinates. Of course, the shape of the PSF changes a little within the FOV and the algorithms have to take into account of this fact, but the symmetry is almost maintained.

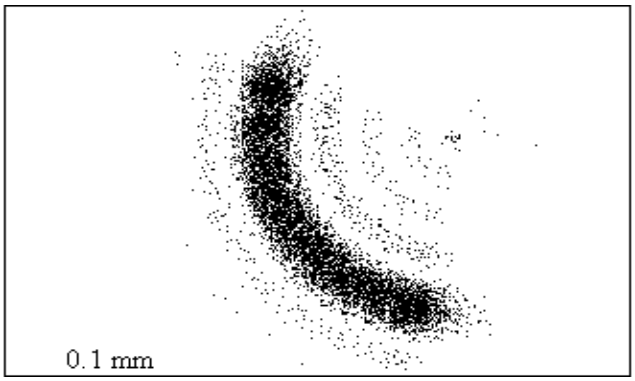

Fig. 7 – PSF from a FOV at 120° from that of Fig. 6

The study was done using the facilities of the optical design package "PROGET"® developed by Officine Galileo.

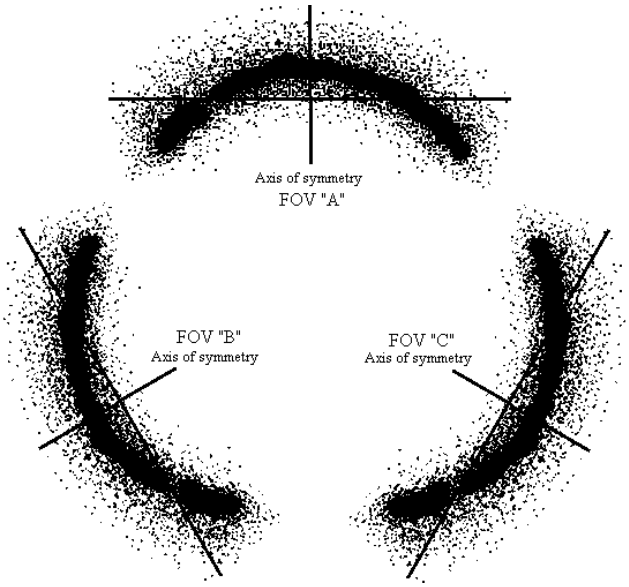

Fig. 8 – PSFs of three different FOVs, A, B and C.

The mirror-block assembly, whose positioning will be defined accordingly to the Schmidt-Cassegrain catadioptric lenses logic, will be designed as the FOV aperture will be defined, while the three baffles mechanisms (one for each FOV), which contains the *shutter closures*, will be designed as a function of the *stray light* decreasing, and of the minimum *cut-off* angle with respect to the optical axis, for the three main bodies of Sun, Earth, and Moon.

The proposed lens definition is under advanced study at the site of Officine Galileo of Alenia Difesa in Firenze (Italy), which help with substantial contribution to the study and development of this new star tracker.

3. Field of View Identification

The solution of a Schmidt-Cassegrain catadioptric system with a geometrical partition of the pupil area produces PSFs whose shapes depend on the FOV to which the star belongs. Therefore, in the principal line, it is possible to identify the FOV of provenance from the shape of the PSF because they appear as having an axis of symmetry which is parallel to the tangential plane defined by the Optical Axis and the normal to the mirror and splits the FOV in two symmetrical parts. It is important to outline that the PSF form can be known - a priori - for any point of the field.

The problem of the FOV identification is reduced, therefore, into the equivalent problem of finding the slope of the symmetry axis (one angle, only), which coincide with an eigenvector of the figure inertia tensor *J*. In particular, the axis of symmetry is that associated with the minimum

eigenvalue (see later on) and this can be evaluated, at centroiding stage, in a fast and easy way. This solution is particularly suitable for the pupil area geometrical partition technique. Thus, by varying some optical parameters, it is possible to obtain different interesting shapes for the PSF whose symmetry orientation allows to identify the associated FOV with the star light. Up to now, the most interesting and promising solution is that outputting toric shaped PSFs, as those shown in Figs. 8 and 9.

The orientation of the inertia axes (see Fig. 6), can easily be accomplished by the eigenanalysis of the figure inertia tensor J

$$J = \begin{bmatrix} \sum_i y_i^2 & -\sum_i x_i y_i \\ -\sum_i x_i y_i & \sum_i x_i^2 \end{bmatrix} = \begin{bmatrix} J_1 & -J_{12} \\ -J_{12} & J_2 \end{bmatrix} \quad (1)$$

where the sums are extended to all of the pixels, belonging to the PSF, used for centroiding. The eigenvalues, λ_1 and λ_2, are given by

$$\lambda_a + \lambda_b = \lambda_1 \geq \lambda_2 = \lambda_a - \lambda_b \quad (2)$$

where

$$\begin{cases} 2\lambda_a = J_1 + J_2 \\ 2\lambda_b = \sqrt{J_1^2 + J_2^2 - 2J_1J_2 + 4J_{12}^2} \end{cases} \quad (3)$$

Associated with the λ_1 and λ_2 eigenvalues, there are the eigenvectors

$$\begin{cases} w_1^{\mathrm{T}} = \{J_2 - J_1 - \lambda_b \quad 2J_{12}\} \\ w_2^{\mathrm{T}} = \{J_2 - J_1 + \lambda_b \quad 2J_{12}\} \end{cases} \quad (4)$$

Now, the symmetry axis (eigenvector w_1), which unequivocally identifies the FOV of provenance of the star light, is that associated with the maximum eigenvalue λ_1. In this way, if the eigenvalues λ_1 and λ_2 are *sufficiently* separated, it is possible to discriminate the FOV where the star light come from. It is obvious that a great attention must be given to what *sufficiently* separated means. Most likely, a threshold on their ratio can be the right choice to understand the working limits.

Finally, for the Schmidt-Cassegrain catadioptric system with a geometrical partition of the pupil area solution, the resulting PSF should be designed from the best compromise between the intensity and the minimum number of pixels allowing the FOV identification.

As for the different solution with PSF constrained into different CCD detector areas, even though this solution simply solves the FOV identification, it presents the unacceptable disadvantage of reducing the number of visible stars for each FOV. To overcome this inconvenience and increase the number of observed stars, we could think to reduce the instrument magnitude threshold; however, in this way, the star identification problems would also increase, especially for the most general *lost-in-space* case. For all these reasons, the solution with confined CCD sub-areas, was withdrawn.

Finally, the solution with more CCD detectors (for instance, one for each FOV) was also withdrawn because it implies more than one electro-optics, and this is exactly what it must be avoided, and the reason for which the multi-fields star trackers have been proposed.

4. STAR IDENTIFICATION

As for the star identification process, with data provided by the new StarNav III sensor, an analytical theory was developed in [11] to evaluate the occurrence frequencies associated with any basic stellar configuration (star pair, star triangle, star cross with *m* branches, etc) which allow us to estimate the reliability associated with any more complex observed star configuration. This analytical approach has led to the development of a new algorithm, called *Pyramid*, to accomplish the star identification process by recognizing a pyramid set of stars, because the frequency of false matches of a four star structure in the catalog is so small (10^{-12}) that the star identification is almost certain.

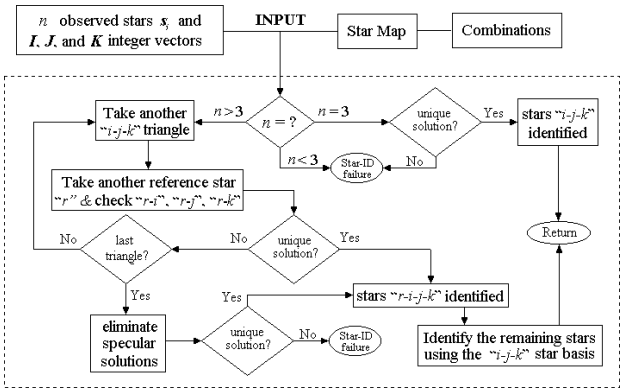

Fig. 9 – Pyramid I Flowchart

The resulting *Pyramid* algorithm, whose flowchart is shown in Fig. 9, is dramatically robust. It's reliability is demonstrated by its capacity to solve the *lost-in-space* case (when the attitude is completely unknown) by identifying the stars in the unreal bad case of 28 observed stars of which only four are real (see Fig. 10), that is, only four stars are present in the catalog. This means that *Pyramid* is capable to identify and discard 24 spikes from this unreal stars scene.

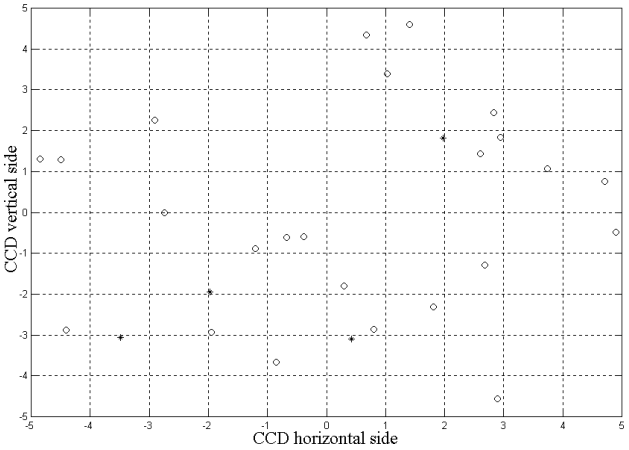

Fig. 10 – Most dramatic star scenario

Most likely, a such extreme situation will never occur during the standard operating modes. Nevertheless, some past experiences as, for instance, that occurred to the star sensor SOAR (which flown on the STS-101 mission), which failed the star identification process because of the great amount of spurious images (spikes due to light reflections originated from space debris expelled from an adjacent experiment), warns us to orient our choice toward more robust methods.

As for the adaptation of the *Search-Less Algorithm* [6] or/and the *Spherical-Polygon Search* [8-9], (both of which are based on the *k*-vector range searching approach), to StarNav III, some drawbacks arise. *Search-Less Algorithm* has already been extended to multiple FOV star trackers, however it is less robust than *Pyramid*, and the *Spherical-Polygon Search* has not been extended to multiple FOV star tracker because it is based on a suboptimal multidimensional *k*-vector. At the present stage, three different approaches are under analysis to extend the *k*-vector technique to multidimensional data. These different approaches, presently at a development stage, will be published soon.

Pyramid I algorithm has been extended to the Multiple-FOV star tracker using standard C language, getting the code *Pyramid III*. The performances of *Pyramid III* code are really impressive in accuracy, speed, and robustness.

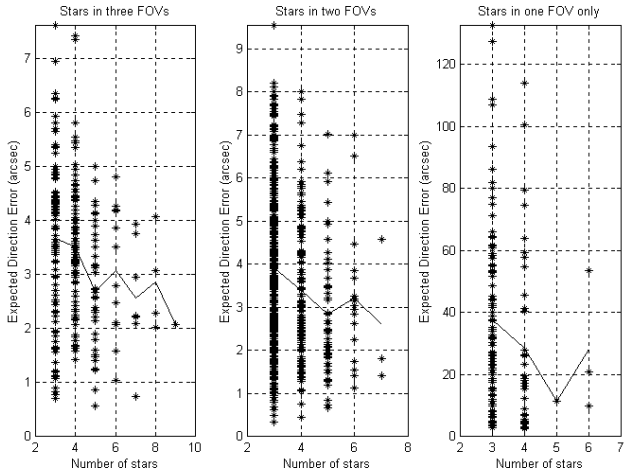

Fig. 11 – Accuracy test results for *Pyramid III*.

In Fig. 11 the accuracy results, obtained by 10,000 random numerical tests, are shown. The figure shows the accuracy in the three cases of all the observed stars in one, two, and three FOVs, respectively.

The gain in term of accuracy (exactly, the expected direction error, which is proportional to the maximum attitude error) is more than one order of magnitude when stars appears in two or more FOVs with respect to stars in one FOV only, as for instance for standard single-FOV star trackers.

5. Optical Axis Offset Computation

In order to keep the accuracy promised in Fig. 11, the location of the Optical Axis (OA) in the CCD system of coordinates, must be precisely estimated. Hereafter, the algorithm developed in [16], which has the purpose of finding accurate values of the OA positioning offsets (the focal length is here supposed to be well known), is summarized. The method solves the problem by least squares technique and uses iterative procedure. The observed star direction b_i, is given by

$$b_i = \frac{1}{\sqrt{(x_0 - x_i)^2 + (y_0 - y_i)^2 + f^2}} \begin{Bmatrix} x_0 - x_i \\ y_0 - y_i \\ f \end{Bmatrix} \tag{5}$$

where f is the known focal length, and $[x_0,y_0]$ are the unknown OA offsets to be determined. The invariance of the observed directions, with respect to different reference systems, allows us to write

$$r_i^{\mathrm{T}} r_j = b_i^{\mathrm{T}} b_j = \frac{c_{ij}}{c_i c_j} = g_{ij}(x_0, y_0) \tag{6}$$

$(i, j = 1, \ldots, n; i \neq j)$ where r_i is the reference direction (the catalog star corresponding to b_i) and where

$$\begin{cases} c_{ij} = (x_0 - x_i)(x_0 - x_j) + (y_0 - y_i)(y_0 - y_j) + f^2 \\ c_i = \sqrt{(x_0 - x_i)^2 + (y_0 - y_i)^2 + f^2} \\ c_j = \sqrt{(x_0 - x_j)^2 + (y_0 - y_j)^2 + f^2} \end{cases} \quad (7)$$

The unknowns can be linearized as

$$x_0 = \hat{x}_0 + \Delta x_0, \quad \text{and} \quad y_0 = \hat{y}_0 + \Delta y_0 \quad (8)$$

and the system of Eq. (6) can be re-written as

$$R_{ij} = r_i^{\mathrm{T}} r_j = g_{ij}(\hat{x}_0, \hat{y}_0) + \begin{bmatrix} \frac{\partial g_{ij}}{\partial x_0} & \frac{\partial g_{ij}}{\partial y_0} \end{bmatrix} \begin{Bmatrix} \Delta x_0 \\ \Delta y_0 \end{Bmatrix} \quad (9)$$

for any *i-j* star pair. This implies that the system of Eq. (6) can be written in the more compact form

$$R = G + J \begin{Bmatrix} \Delta x_0 \\ \Delta y_0 \end{Bmatrix} \quad (10)$$

where R and G are vectors, and J the Jacobian rectangular matrix. The least-square solution simply gives

$$\begin{Bmatrix} \Delta x_0 \\ \Delta y_0 \end{Bmatrix} = \left[J^{\mathrm{T}} J \right]^{-1} J^{\mathrm{T}} R \quad (11)$$

Numerical results of the method, which allows an iterative solving procedure, and the convergence speed are given in Fig. 12 for a single FOV.

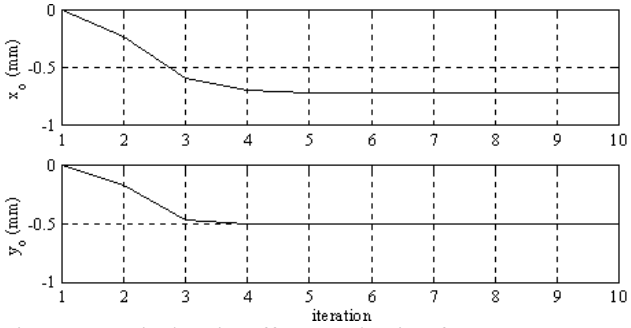

Fig. 12 – Optical Axis Offsets evaluation for *StarNav I.*

6. CENTROIDING

Centroiding is a process that, like the attitude estimation task, is wished to be executed in a fast and accurate way.

6.1 Centroiding speed

As for the speed, two fast approaches have been proposed which, by scanning all the CCD pixels just once, finds all the needed info where the star spot lights are located. The first method accomplished the task by introducing two integer vectors, I_h and I_v of n_h and n_v elements, respectively, where n_h and n_v are the number of the CCD horizontal and vertical pixels, respectively. These two vectors keep record of the location of the relative maximum in the corresponding row/column. This means, for instance, that if the brightest element of the 5th row is located at the 123th column and the brightest element of the 77th column is located at the 31st row, then

$$I_v(5) = 123, \quad \text{and} \quad I_h(77) = 31 \quad (12)$$

These two integer vectors allows, then, a fast way to find out all the n first brightest pixels (most likely, where the star spot lights are located) on the CCD, by avoiding subsequent CCD pixel scans, which are, in turn, time consuming.

The second approach, called "Run Length Encode" (RLE) method, scans the entire image just once in order to find clusters of adjacent pixels which lies in the same image row and then merges the clusters if they are adjacent. When no more adjacent clusters remain to be merged, the blocks of adjacent pixels are isolated and then the centroiding process can be applied.

6.2 Centroiding accuracy

As for the accuracy of the centroiding problem, that is, to an accurate determination of the star light directions, it is important to outline that this process highly depends on the shapes of the CCD PSF. Since complex PSF shapes (as those proposed for StarNav III) are not well fitted by square or rectangular masks, a recent study has been carried out, which introduces two fundamental new approaches to tackle this problem.

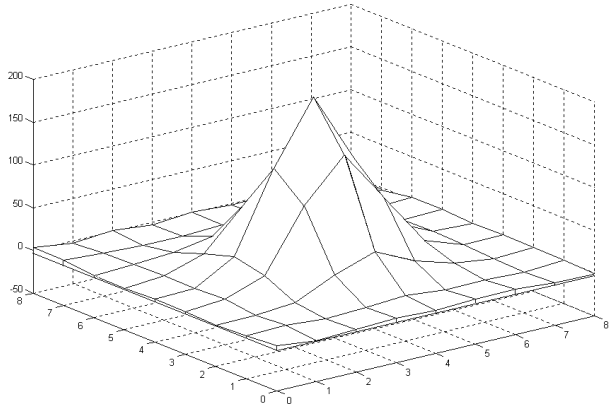

Fig. 13 – Edge noise effects on centroiding using standard squared masks

The first new aspect consists of increasing the centroiding accuracy by using masks of assigned shapes (rectangular, ellipsoidal masks) which, relative to the standard squared masks, presents the advantage (see Fig. 13) to minimize the bad contributions due to electronic noise variation in the pixels located far from the PSF center of mass (centroiding). A second important improvement is related to the use of recursive functions (functions which call themselves), which are standard for C programming. These functions, which differ one from another for different constraint philosophies, allow the identification of any complex PSF forms, even more complex to that presented in Figs. 5-8, as the solution for StarNav III. One philosophy, for instance, could be represented to build up a recursive function that identify all the pixels with gray tone over a given threshold magnitude and constrained to be within an ellipsoidal mask.

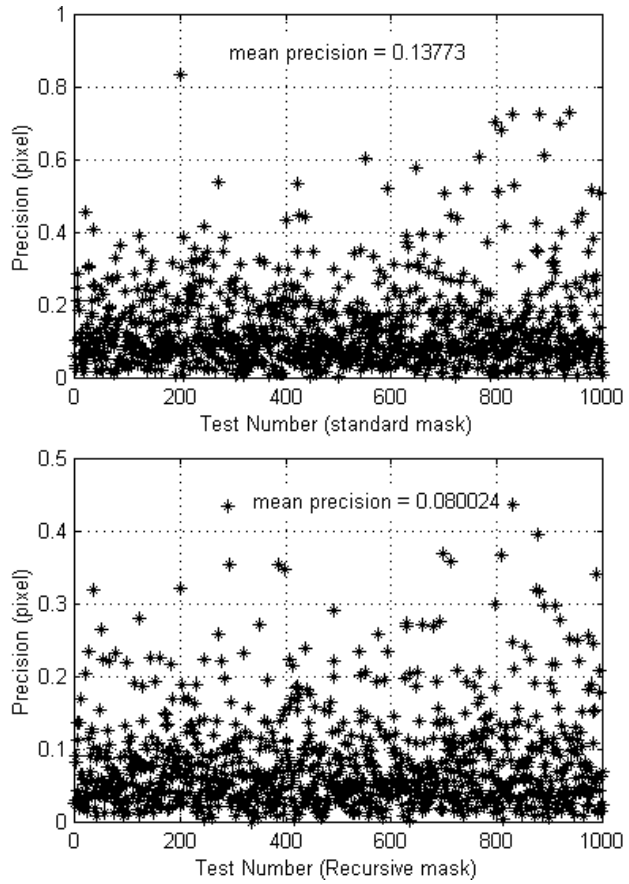

Fig. 14 – Centroiding accuracy test results

In Fig. 14, the gain obtained by numerical test using a such recursive function is compared to a squared-mask standard approach. The figure shows an increase of the centroiding accuracy from 0.138 to 0.080 mean values, that implies a 40% gain in accuracy.

7. MISALIGNMENTS

Due to many different causes, as for instance thermal and mechanical effects, the orientation of the FOV system of coordinates with respect to the body reference frame varies. Therefore, it is important to develop some methodologies which provide us a tool to update these rotation matrices. This important problem has been solved for both the practical different cases that may occur: for the *small* and for the *large* misalignment cases. Misalignments, even small ones, imply the computation of two rigid rotation matrices. This problem, which has already been solved in [12], can easily be accomplished on-board by means of two least-square method, that allows the *misalignment* matrices updating for the two cases of *small* and *large* misalignments. Small means that the misalignment is so small that the star identification process can still be accomplished using all the three FOV stars, while large means that the star identification process can be accomplished using only each FOV separately.

7.1 Small Misalignment

Let "A" be the non deflected FOV. Then, for the first method the variation from the nominal "B"-FOV attitude, can be described by a small rotation matrix

$$M_B \cong I_{3\times 3} - \tilde{\theta}_B \tag{13}$$

Based on this linearization, the least-square solution for θ_B is simply given by

$$\theta_B = \left[C^{\mathrm{T}} C\right]^{-1} C^{\mathrm{T}} \left[R - B\right] \tag{14}$$

where $R^{\mathrm{T}} \equiv \left\{ \cdots \quad r_k^{(B)\mathrm{T}} R_A \quad \cdots \right\}$, $B^{\mathrm{T}} \equiv \left\{ \cdots \quad b_k^{(B)\mathrm{T}} A_B B_A \quad \cdots \right\}$, and $C^{\mathrm{T}} \equiv \left\{ \cdots \quad -\widetilde{A_B r_k^{(B)}} B_A \quad \cdots \right\}$, and where

$$\begin{cases} R_A \equiv \left[r_1^{(A)} \quad r_2^{(A)} \quad \cdots \quad r_{n_A}^{(A)} \right] \\ B_A \equiv \left[b_1^{(A)} \quad b_2^{(A)} \quad \cdots \quad b_{n_A}^{(A)} \right] \end{cases} \tag{15}$$

indicate the reference identified stars (r_i), and the observed stars (b_i) for the "A"-FOV, respectively, and where

$$\begin{cases} R_{BC} \equiv \left[R_B \quad R_C \right] \\ B_{BC} \equiv \left[B_B \quad B_C \right] \end{cases} \tag{16}$$

are the reference and the observed stars for the misaligned and deflected FOVs.

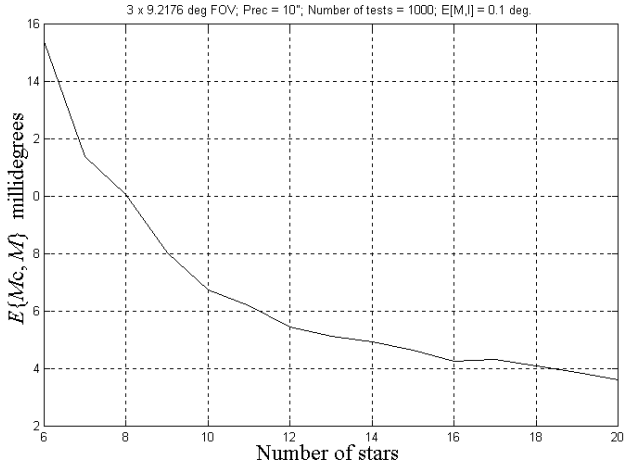

Fig. 15 Numerical test results for small misalignment (0.1°).

7.2 Large Misalignment

The second method, which hold for any misalignment value, implies that the star identification process can be performed separately, for each FOV. Let "A" be the non deflected FOV, then the misalignment M_B of the B-FOV can be evaluates as follows. In the ideal case, it is possible to write

$$B_A = A_A R_A \quad \text{and} \quad M_B A_B B_B = A_A R_B \tag{17}$$

This allows us to evaluate the attitude of the A-FOV, that is, getting A_A, and then to evaluate the misalignment M_B of the B-FOV directly from the the second equation. In other words, once the matrix A_A is computed with the first equation, we will have to solve the Wahba's problem

$$\overline{B}_B = M_B^{\mathrm{T}} \overline{R}_B \tag{18}$$

where

$$\overline{B}_B = A_B B_B \quad \text{and} \quad \overline{R}_B = A_A R_B \tag{19}$$

which solves the problem for large misalignment.

Results and tests for the two methods to evaluate the mirror misalignment, are given in Figs. 15 and 16, respectively.

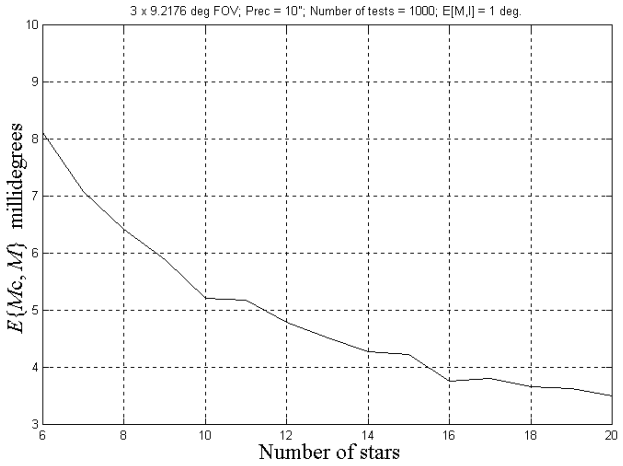

Fig. 16 Numerical test results for large misalignment (1°).

Both approaches have been coded in MATLAB and tested. At the present stage, these codes are under translation into C language.

8. ATTITUDE ESTIMATION

From the optimal attitude estimation problem, the proposed instrument does not present any particular constraint with respect to standard star trackers.

When the attitude data set consists of directions measured by a wide-FOV star tracker, only, it is common to optimally estimate the spacecraft attitude (Wahba problem) using constant relative weights for all the observed directions. This implies that almost all of the existing optimal attitude determination codes can be simplified, thus implying faster codes. However, this choice is a mistake for the accuracy because brighter stars have better signal to noise ratio and less susceptibility to change transfer efficiency losses.

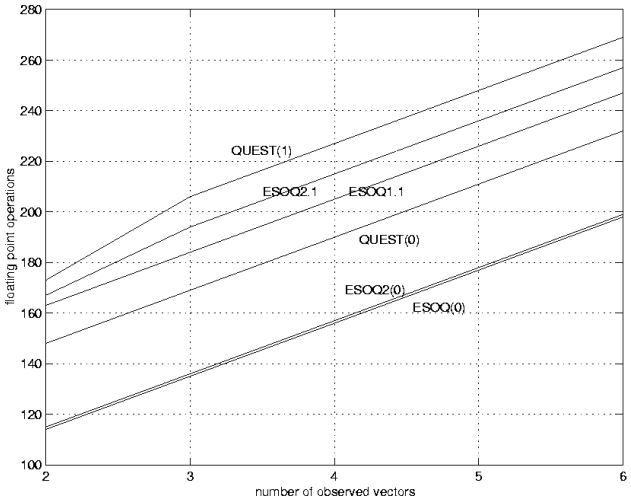

Fig. 17 – Speed test among QUEST, ESOQ-1, and ESOQ-2

This implies, that our choice should be directed toward the fastest optimal approaches. To this end, the study in [15] has demonstrated that ESOQ-1 [13] and ESOQ-2 [14], together with their linearized fast versions ESOQ-1.1 and ESOQ-2.1, are the best choice for star trackers. In particular, Fig. 17 illustrates the speed tests performed in [15] among the fastest optimal algorithms, as a function of the observed directions (in this case, star directions).

ESOQ-1 and ESOQ-2 have been translated to C from the original MATLAB code, and they are ready to be included into a robust and complete StarNav III software package for the autonomous navigation.

Nevertheless, from a theoretical point of view, it is possible to use any one of the existing methods for optimal estimation of the spacecraft attitude, based on the Wahba's optimality criterion. For instance, it is possible to adopt standard known approaches, as *q*-method, SVD, or QUEST.

9. ISS POSITIONING

As for the operating times, they are highly dependant on the orbit, on the nominal onboard orientation, and on the spacecraft attitude stabilization. Geometrical constraints may arise from a limited available open sky.

As for the location position of the Multi-FOV Star Tracker StarNav III on the International Space Station, it is possible to give some suggestions, only. The exact location of the instrument on the ISS will be the subject of future study. The location, obviously, will be determined based on the available spaces, and on the ISS orbital and mechanical constraints. The Express Pallets, close to the Columbus module, have both the right orientation (toward zenith) and the an open sky free from the power arrays, which shouldn't hide any of the sensor FOVs. A deeper study, however, would imply an estimation of the operating times for all of the possible and different configurations.

At the present stage of knowledge, some other preliminary hypotheses can also be given. Available locations for the sensor positioning, can be found on the Express Pallets (see Fig. 18), located at:

1) Starboard Payload Attach Sites (S3 segment truss),
2) JEM Exposed Facility Sites, and
3) Columbus Laboratory External Payload Facility.

Obviously, the choice of the Pallet (or a subpart of it) highly depends on the open sky availability for the sensor FOVs. In particular, it is important that the open sky is directed toward zenith (to avoid Earth presence), even though obscurations will better test the system critical aspects.

Based on the compact instrument dimensions, (see later), provided that the electrical, mechanical, and thermal interfaces are satisfied, the proposed instrument can share the Express Pallet Adapter with another payload. The *Express Pallets* have all the resources for payload power supply, and data transmission.

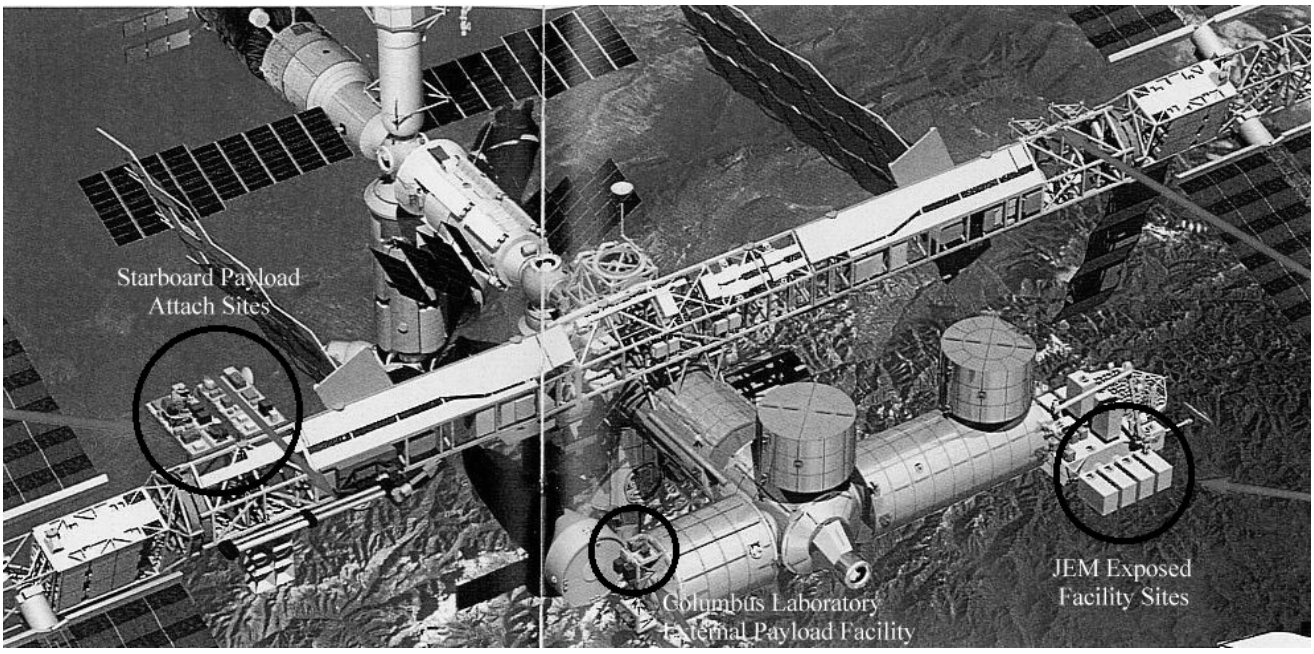

Fig. 18 - StarNav III proposed locations on ISS

Just to give an idea of the StarNav III mechanical and electrical parameters, a rough estimation of them is listed hereafter:

- Mass: about 5 Kg, tbc.
- Power: 15 Watts, tbc.
- Volume: 300×300×300 (mm^3), tbc.
- Electrical Interface: MIL-STD-1553B, or Ethernet.

11. CONCLUSIONS

This paper shows some of the main results obtained in the feasibility study of the new multi-fields StarNav III star tracker which is funded by Italian Space Agency as one of the possible Italian experiments, to be tested onboard the International Space Station. Some optical solutions have been proposed to solve the fundamental problem of focusing star images coming from three orthogonal fields of view onto a single CCD/CMOS imager. These solutions, which present different advantages/disadvantages (as a function of the cost, the complexity, and the integration difficulty factors), include chromatic, monochromatic standard, and monochromatic with PSF shape modeling solutions.

The latter solution is, up to now, the most promising even though, for this solution, the problem of FOV identification arises. This paper shows an easy way to solve this problem by evaluating eigenvalues and eigenvectors of the figure inertia tensor of the PSF.

Many new ideas are presented for the centroiding, star identification, mirror misalignment, and attitude estimation problems. Most of the presented new approaches can directly be imported in almost all of the standard CCD single-FOV star trackers. This implies an increase in both accuracy and computational speed that can be achieved by the data processing associated with the optimal estimation of spacecraft attitude.

REFERENCES

[1] Mortari, D., Pollock, T.C., and Junkins, J.L. "Towards the Most Accurate Attitude Determination System Using Star Trackers," Advances in the Astronautical Sciences, Vol. 99, Pt. II, pp. 839-850, 1998.

[2] Szczepaniak, R., Bailly, M., Duchon, P., Albukerque, J., and Krebs, J. "Design of a New Attitude Measurement and Control System for Satellite in Geosynchronous Orbit Using Stars Detection Reference," Paper IAF-87-54, 38th Congress of the International Astronautical Federation, October 10-17, 1987, Brighton, United Kingdom.

[3] Junkins, J.L., and Pollock, T.C., "Micro Star Tracker and Attitude Determination System," Third International Symposium on Reducing the Cost of Spacecraft Ground Systems and Operations, Tainan, Taiwan, March 22-24, 1999.

[4] Ju, G., Pollock, T., and Junkins, J.L. "Digistar II Micro-Star Tracker: Autonomous On-Orbit Calibration and Attitude Estimation," AAS/AIAA Astrodynamics Specialist Conference, Girdwood, Alaska, August 16-18, 1999.

[5] Junkins, J.L., Ju, G., Kim, H., and Pollock, T. "Digistar: A Low Cost Micro Star Tracker," AIAA '99 Space Technology Conference and Exposition, Albuquerque, NM, September 28-30, 1999.

[6] Mortari, D. "Search-Less Algorithm for Star Pattern Recognition," *Journal of the Astronautical Sciences*, Vol. 45, No. 2, April-June 1997, pp. 179-194.

[7] Mortari, D., and Neta, B. "*k*-vector Range Searching Techniques," Paper AAS 00-128 of the 10th Annual AIAA/AAS Space Flight Mechanics Meeting, Clearwaters, FL, Jan. 23-26, 2000.

[8] Mortari, D. "SP-Search: A New Algorithm for Star Pattern Recognition," Advances in the Astronautical Sciences, Vol. 102, Pt. II, pp.1165-1174, 1999.

[9] Mortari, D., and Junkins, L.J. "SP-Search Star Pattern Recognition for Multiple Fields of View Star Trackers," Paper 99-437 of the AAS/AIAA Astrodynamics Specialist Conference, Girdwood, AK, August 15-19, 1999.

[10] Ju, G., Kim, Y.H., Pollock, C.T., Junkins, L.J., Juang, N.J., and Mortari, D. "Lost-In-Space: A Star Pattern Recognition and Attitude Estimation Approach for the Case of No A Priori Attitude Information," Paper of the 2000 AAS Guidance & Control Conference, Breckenridge, CO, Feb. 2-6, 2000.

[11] Mortari, D., Junkins, L.J., and Samaan, M.A. "Lost-In-Space Pyramid Algorithm for Robust Star Pattern Recognition", Paper AAS 01-004 Guidance and Control Conference, Breckenridge, Colorado, 31 Jan. - 4 Feb. 2001.

[12] Mortari, D., and Angelucci, M. "Star Pattern Recognition and Mirror Assembly Misalignment for DIGISTAR II and III Star Sensors," Advances in the Astronautical Sciences, Vol. 102, Pt.II, pp.1175-1184, 1999.

[13] Mortari, D. "ESOQ: A Closed-Form Solution to the Wahba Problem," *Journal of the Astronautical Sciences*, Vol. 45, No. 2, April-June 1997, pp. 195-204.

[14] Mortari, D. "Second Estimator of the Optimal Quaternion," *Journal of Guidance, Control, and Dynamics*, Vol. 23, No. 5, Sept.-Oct. 2000, pp. 885-888.

[15] Markley, L.F., and Mortari, D. “New Developments in Quaternion Estimation from Vector Observations,” Paper AAS 00-266 of the Richard H. Battin Astrodynamics Symposium Conference, Texas A&M University, College Station, TX, March 20-21, 2000, Vol. 106, pp. 373-393.

[16] Samaan, M.A., Mortari, D., and Junkins, L.J., “Recursive Mode Star Identification Algorithms”, Paper AAS 01-194 of the Space Flight Mechanics Meeting, Santa Barbara, CA, 11-14 February, 2001.

Daniele Mortari *is Assistant Professor at the Aerospace School of Engineering of the University ”La Sapienza” of Rome (Italy), and Visiting Associate Professor at Texas A&M University (TX, U.S.A.). He attended the Nuclear Engineering and Aerospace School of Engineering, both at University of Rome, Italy. He was trained at Goddard Space Flight Center (NASA) for Attitude and Orbit Control Systems. He joined the San Marco Project and cooperated in the activities for San Marco spacecraft, for which he was awarded in 1983. As a researcher, the most of its contribution is given in the fields of attitude determination, attitude dynamics, navigation, data processing (especially in star pattern recognition), and matrix analysis. At the University of Perugia (Italy), he helds the “Aerospace Systems” course. He is the author of more than 50 papers. He is member of the AIAA and AAS.*

Andrea Romoli *graduated in Physics by Florence University in 1973, he is by Officine Galileo since 1973, where he is responsible for Optical Design Department by Officine Galileo since 1975. He is senior optical engineer and his main activities involve feasibility and theoretical studies for space optics, development of new methods and algorithms for optical design and teaching. He is titular of some recent patents, concerning spectrometers of new conception.*